

Figure S1: Intensity fraction distributions of the apparent hydrodynamic radius R_h for 10R5/H₂O/1,2-dichloroethane (lines) and 10R5/D₂O/1,2-dichloroethane (dotted lines) mixtures at fixed copolymer molar fraction ($X_p=0.009$) and different 1,2-dichloroethane concentrations (X_a) at 25 and 35 °C.

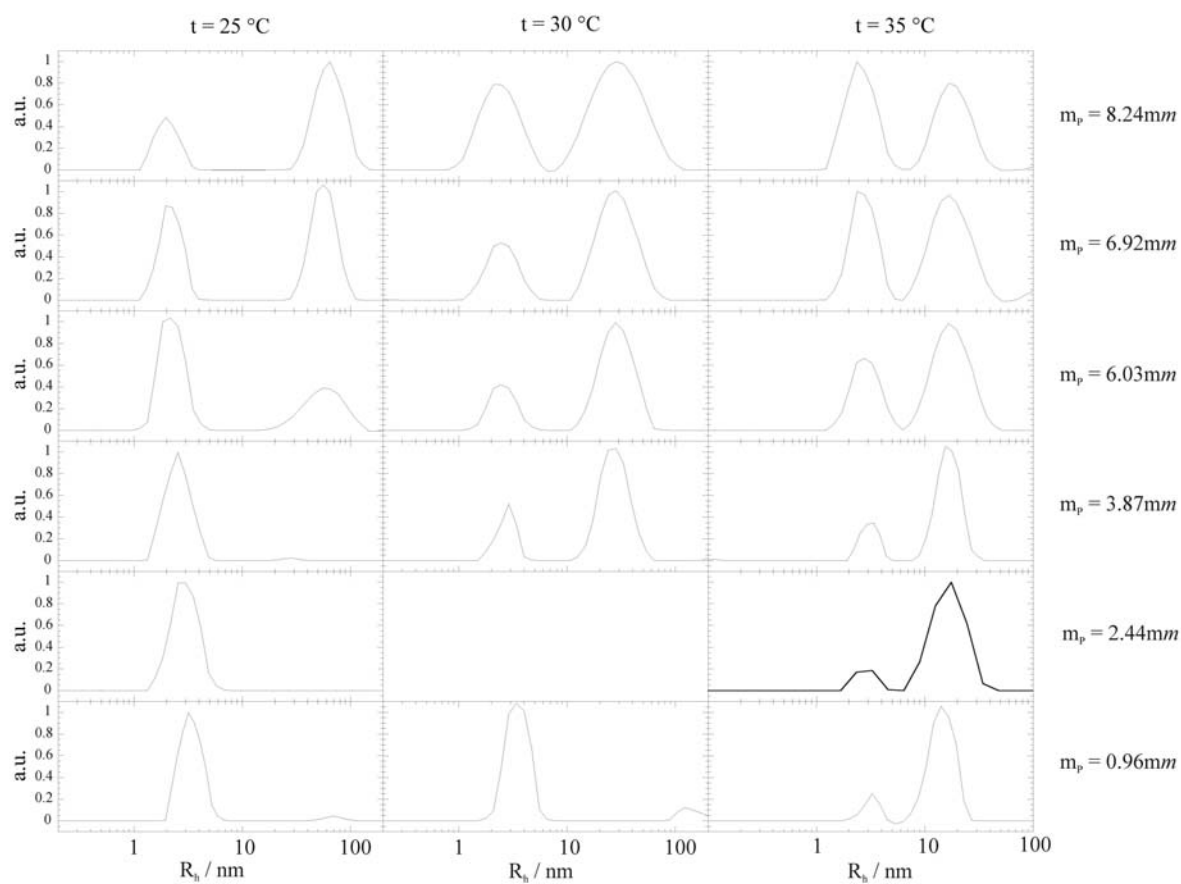


Figure S2. Intensity fraction distributions of the logarithm of apparent hydrodynamic radius for aqueous solutions of copolymer F108 at variable copolymer concentration and temperature.

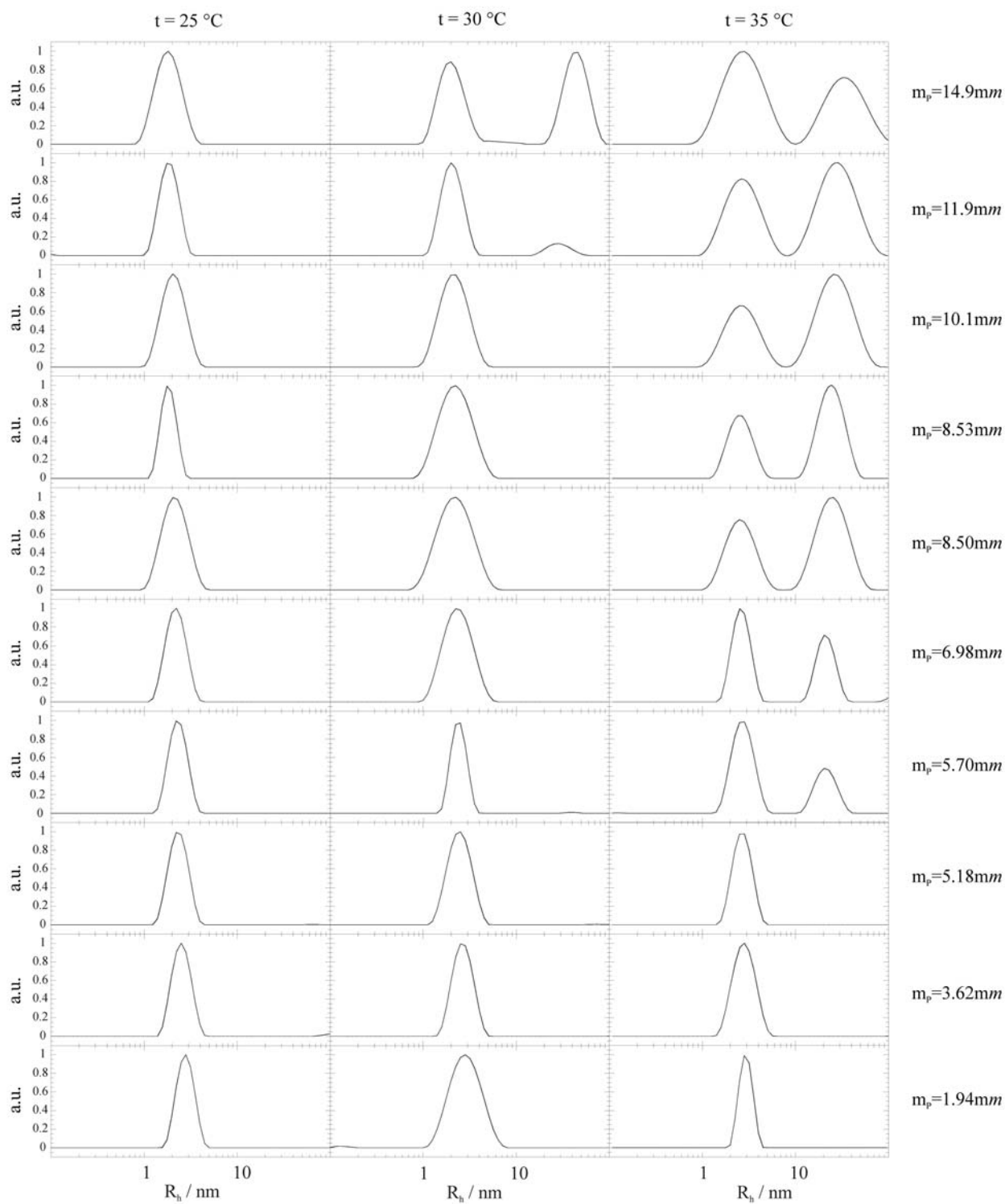


Figure S3. Intensity fraction distributions of the logarithm of apparent hydrodynamic radius for aqueous solutions of copolymer F88 at variable copolymer concentration and temperature.

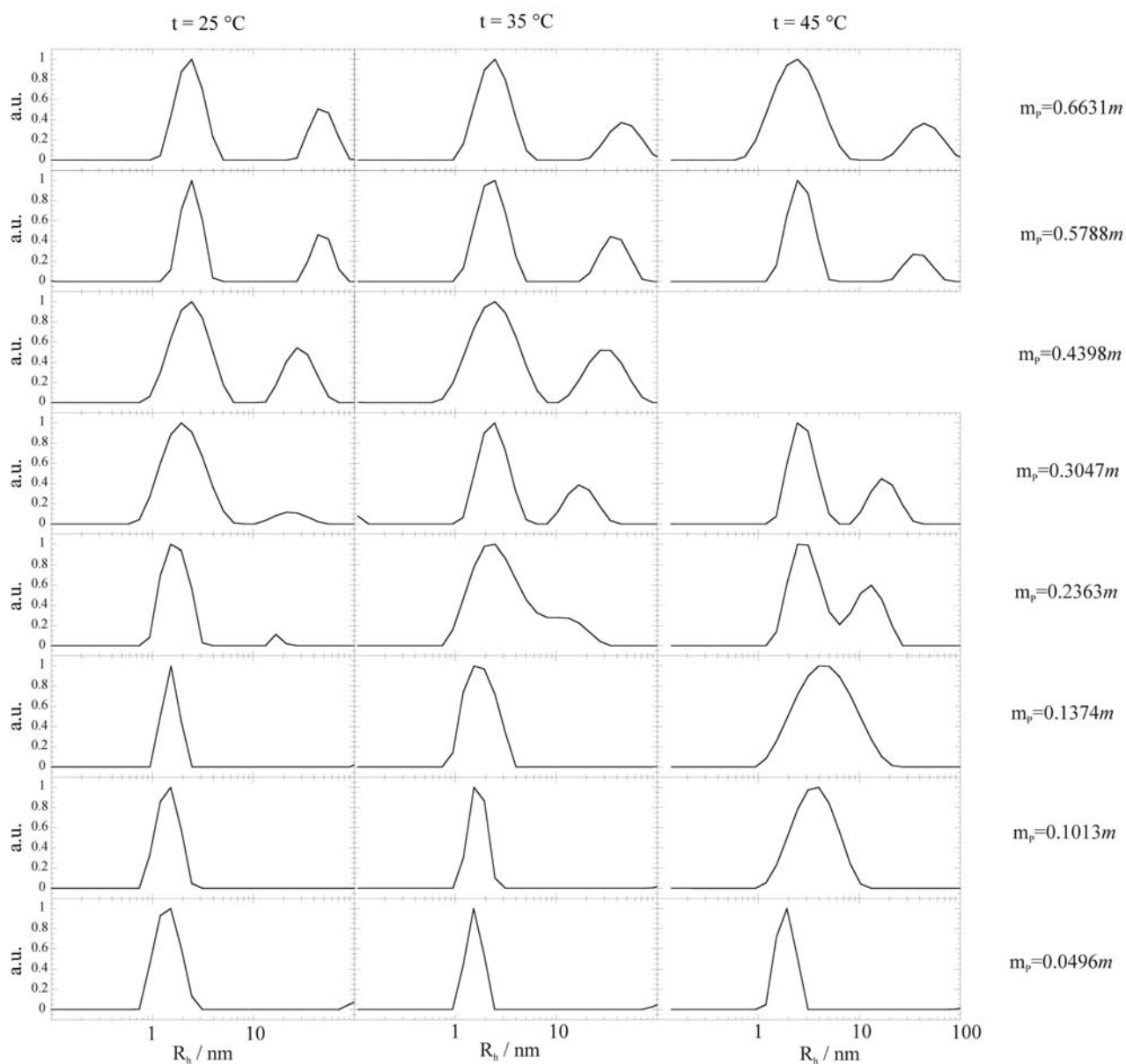


Figure S4. Intensity fraction distributions of the logarithm of apparent hydrodynamic radius for aqueous solutions of copolymer L35 at variable copolymer concentration and temperature.

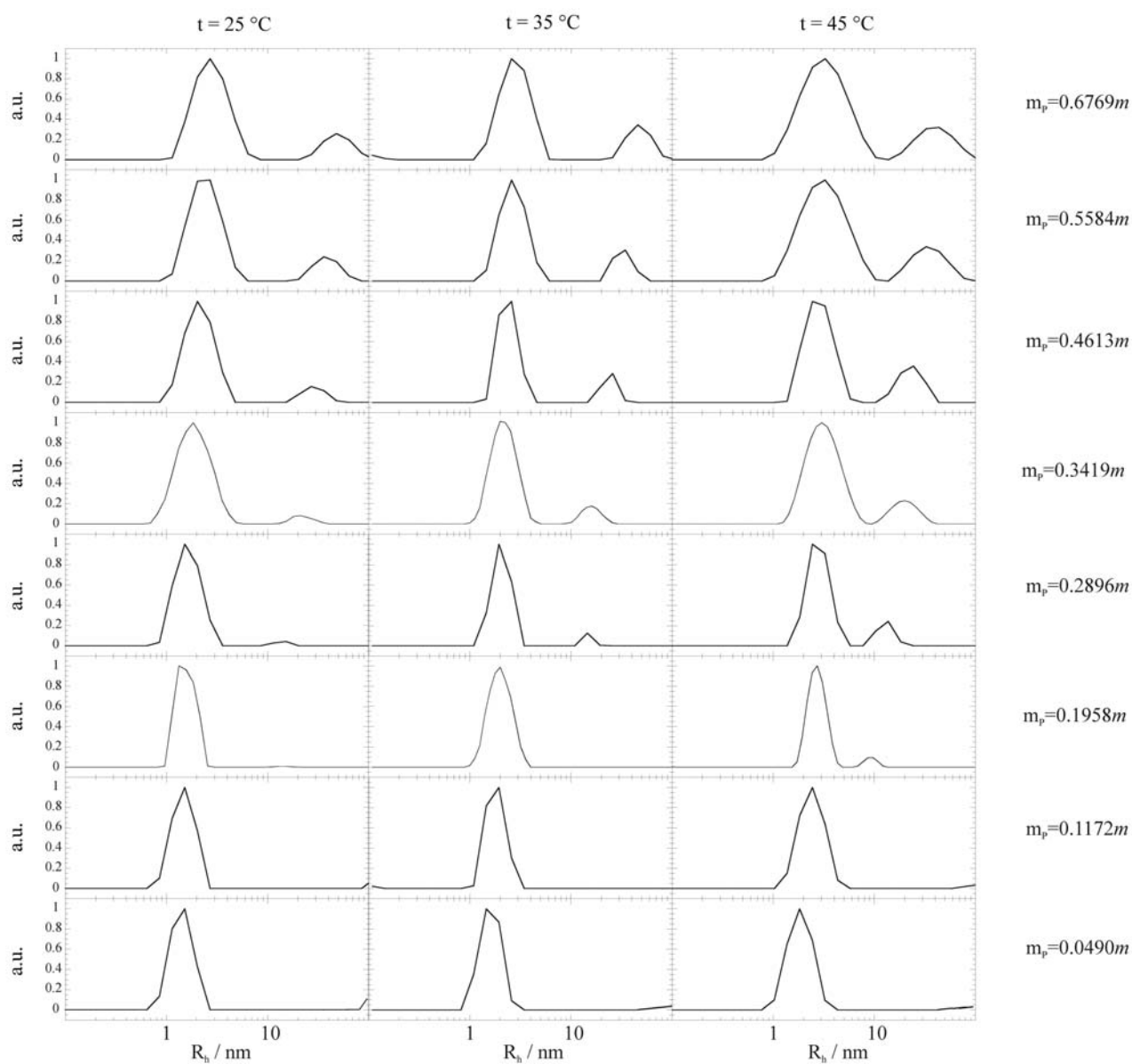


Figure S5. Intensity fraction distributions of the logarithm of apparent hydrodynamic radius for aqueous solutions of copolymer 10R5 at variable copolymer concentration and temperature.

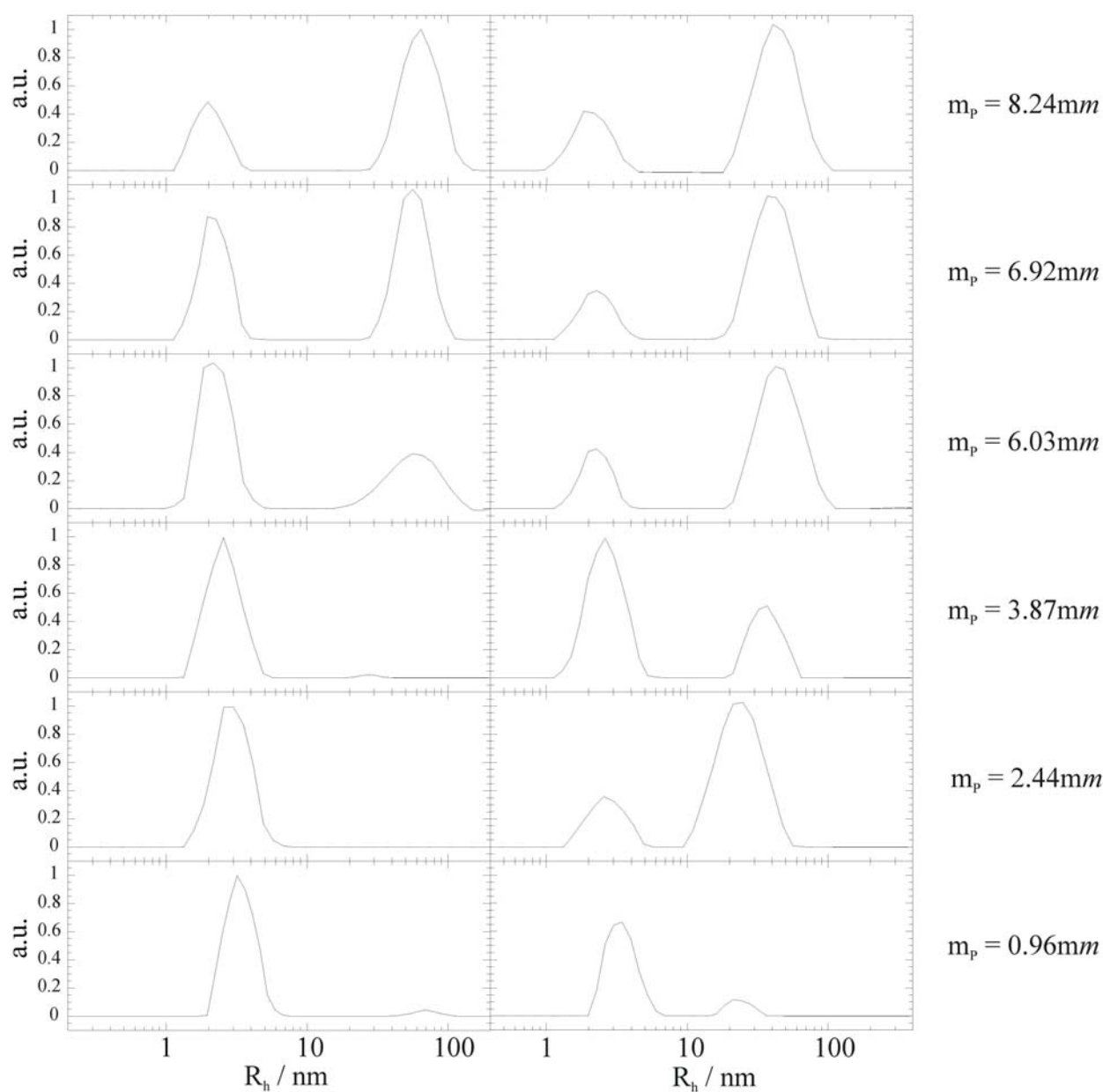


Figure S6. Intensity fraction distributions of the logarithm of apparent hydrodynamic radius for aqueous solutions of copolymer F108 in absence (left) and in presence (right) of 1,2-Dichloroethane 0.1m at variable copolymer concentration and 25 °C.

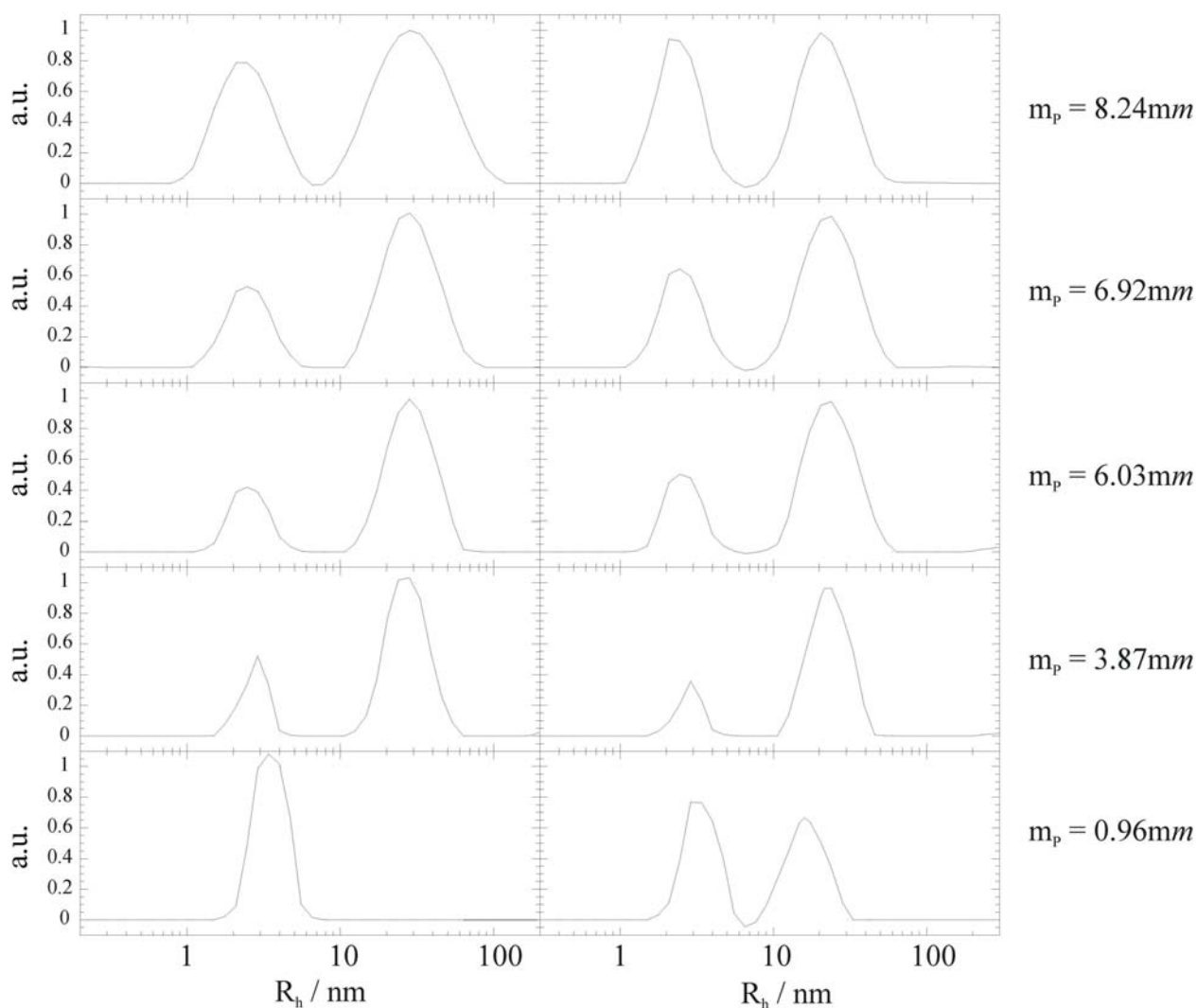


Figure S7. Intensity fraction distributions of the logarithm of apparent hydrodynamic radius for aqueous solutions of copolymer F108 in absence (left) and in presence (right) of 1,2-Dichloroethane 0.1 M at variable copolymer concentration and 30 °C.

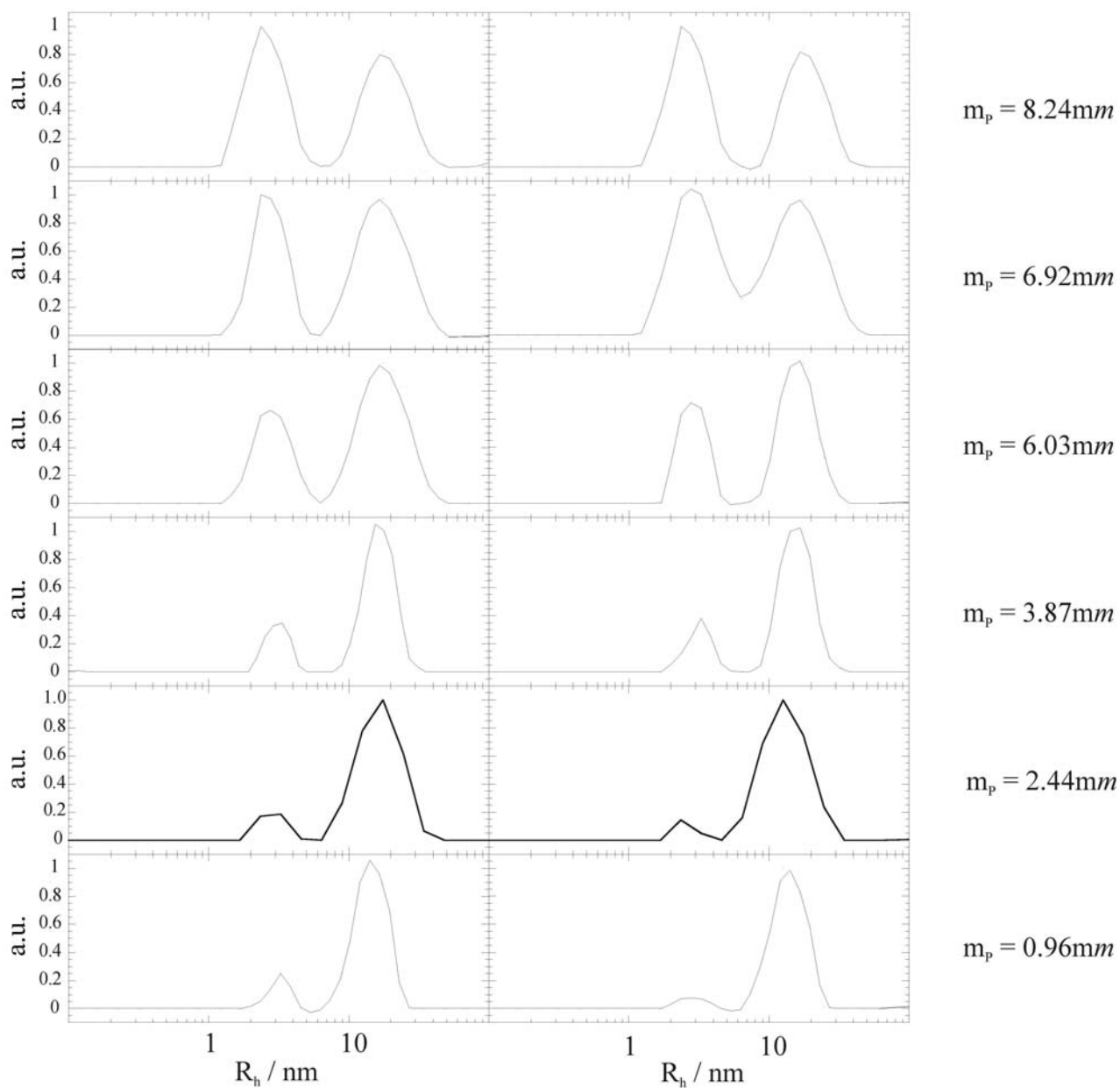


Figure S8. Intensity fraction distributions of the logarithm of apparent hydrodynamic radius for aqueous solutions of copolymer F108 in absence (left) and in presence (right) of 1,2-Dichloroethane 0.1m at variable copolymer concentration and 35 °C.

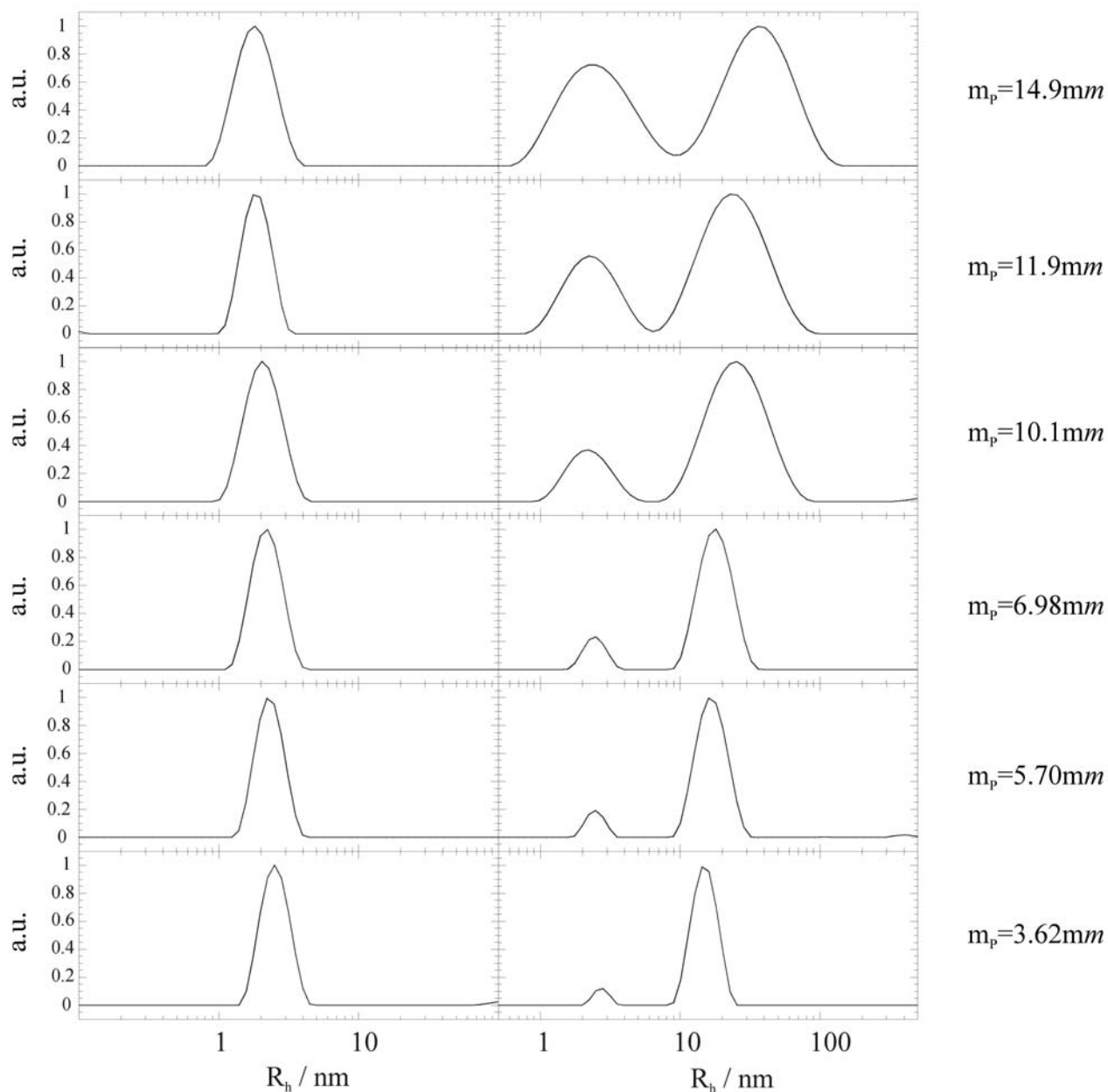


Figure S9. Intensity fraction distributions of the logarithm of apparent hydrodynamic radius for aqueous solutions of copolymer F88 in absence (left) and in presence (right) of 1,2-Dichloroethane 0.1m at variable copolymer concentration and 25 °C.

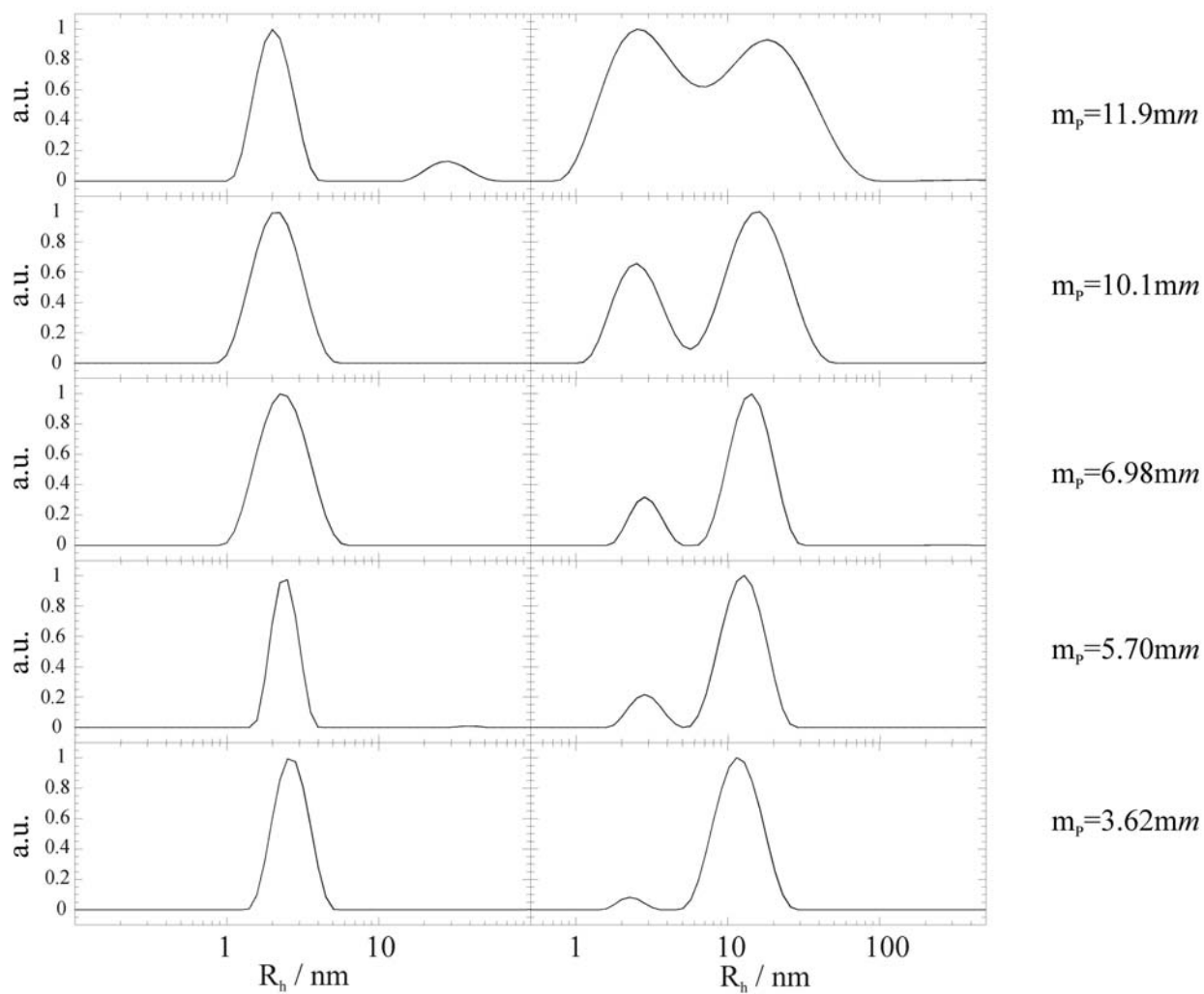


Figure S10. Intensity fraction distributions of the logarithm of apparent hydrodynamic radius for aqueous solutions of copolymer F88 in absence (left) and in presence (right) of 1,2-Dichloroethane 0.1*m* at variable copolymer concentration and 30 °C.

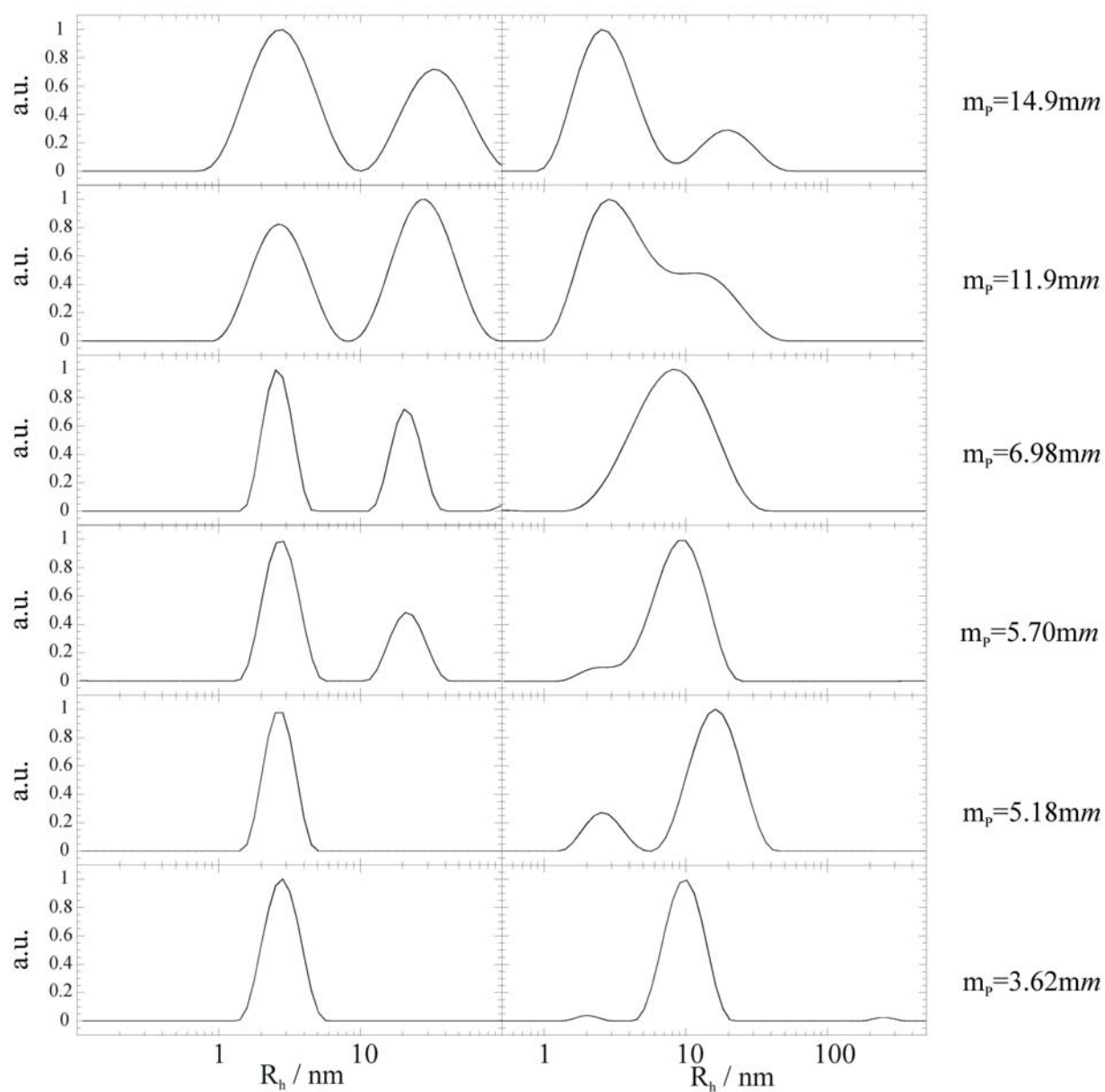


Figure S11. Intensity fraction distributions of the logarithm of apparent hydrodynamic radius for aqueous solutions of copolymer F88 in absence (left) and in presence (right) of 1,2-Dichloroethane 0.1m at variable copolymer concentration and 35 °C.

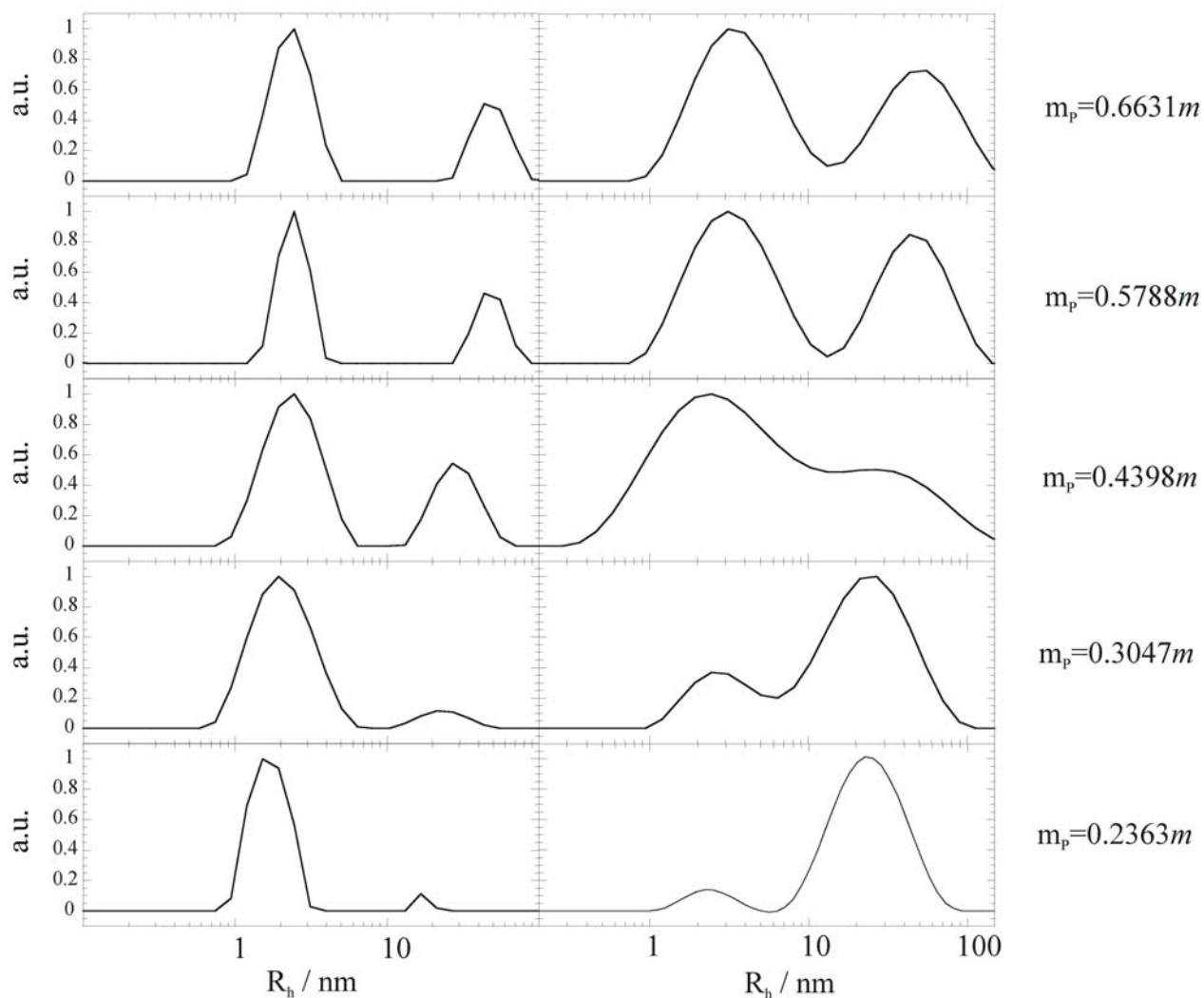


Figure S12. Intensity fraction distributions of the logarithm of apparent hydrodynamic radius for aqueous solutions of copolymer L35 in absence (left) and in presence (right) of 1,2-Dichloroethane $1.2m$ at variable copolymer concentration and 25°C .

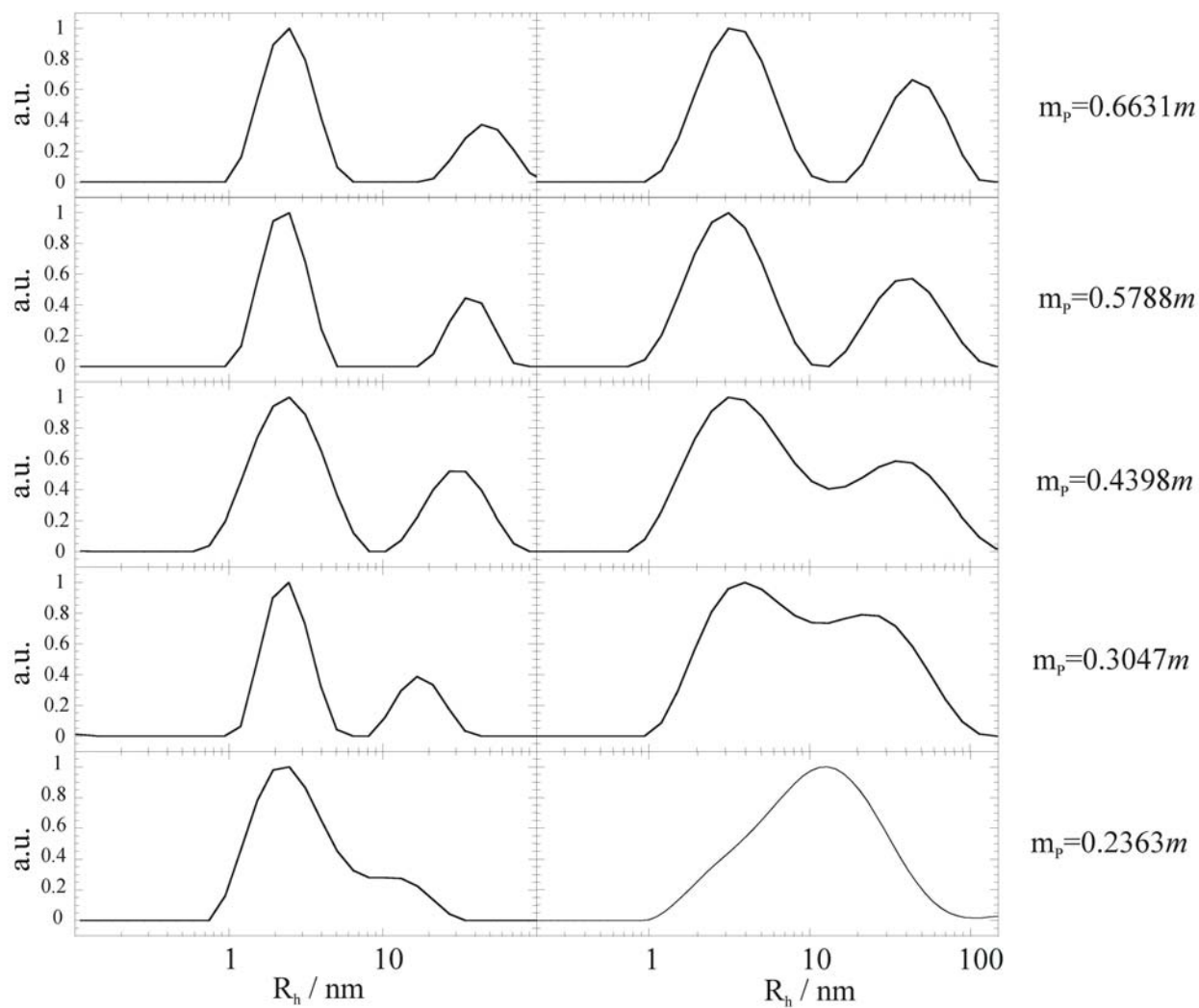


Figure S13. Intensity fraction distributions of the logarithm of apparent hydrodynamic radius for aqueous solutions of copolymer L35 in absence (left) and in presence (right) of 1,2-Dichloroethane $1.2m$ at variable copolymer concentration and 35°C .

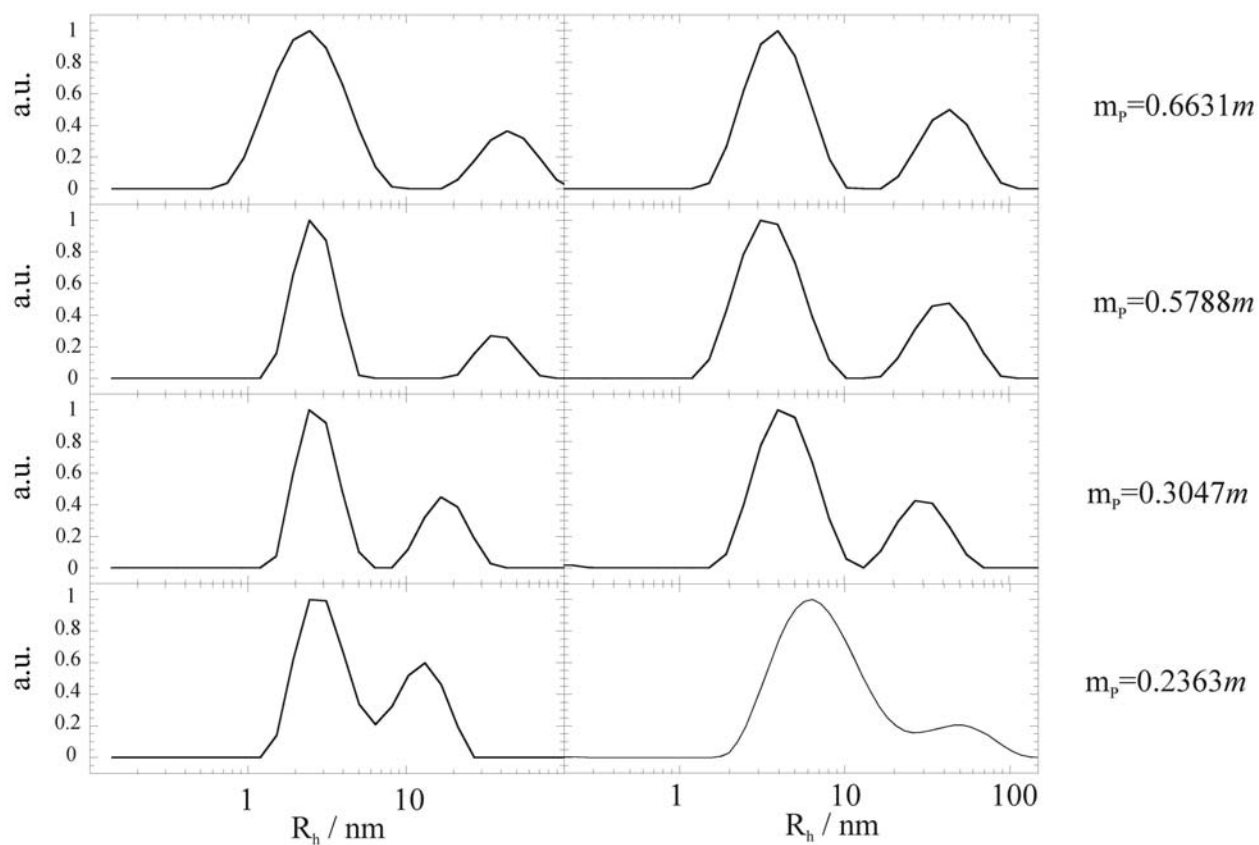


Figure S14. Intensity fraction distributions of the logarithm of apparent hydrodynamic radius for aqueous solutions of copolymer L35 in absence (left) and in presence (right) of 1,2-Dichloroethane $1.2m$ at variable copolymer concentration and 45°C .

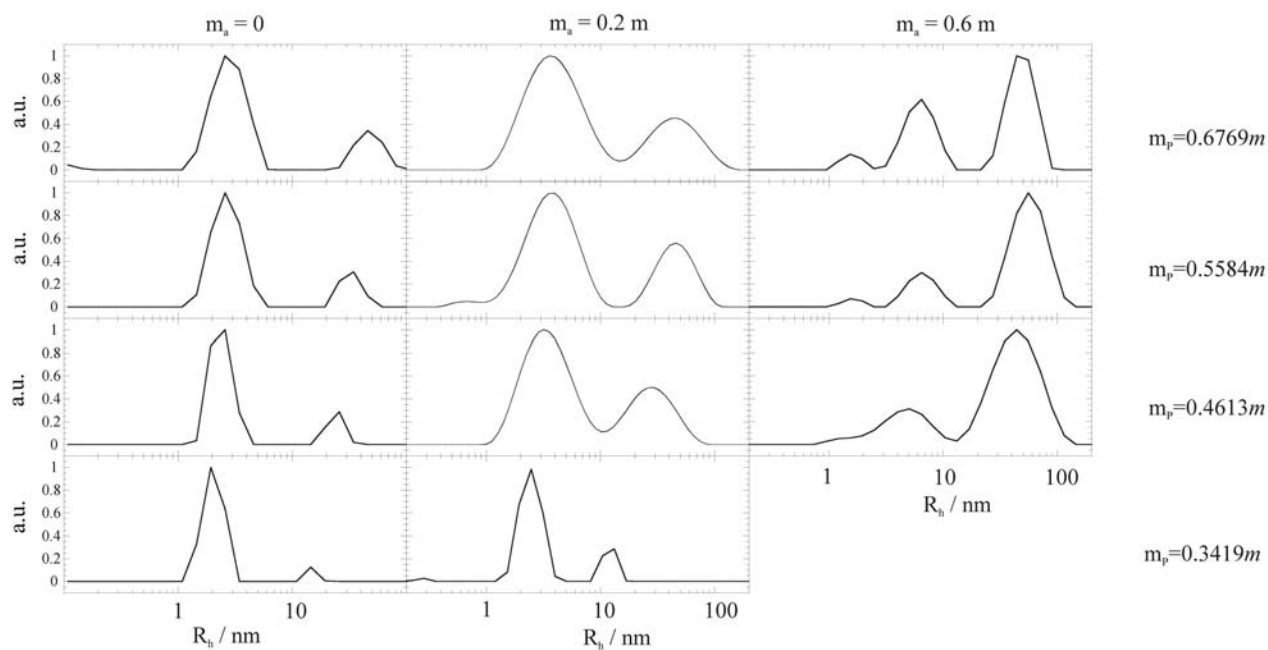


Figure S15. Effect of the copolymer composition on the intensity fraction distributions of the logarithm of the apparent hydrodynamic radius of 10R5 in water and in water+1,2-dichloroethane mixtures at 35 °C.

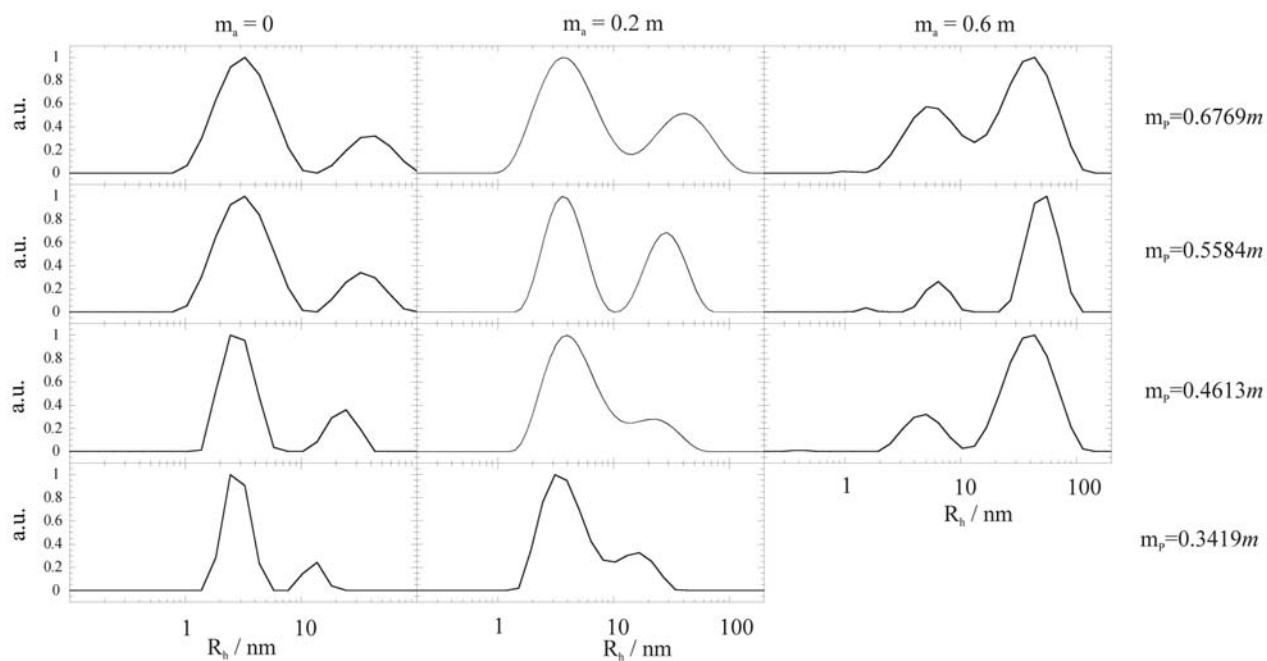


Figure S16. Effect of the copolymer composition on the intensity fraction distributions of the logarithm of the apparent hydrodynamic radius of 10R5 in water and in water+1,2-dichloroethane mixtures at 45 °C.

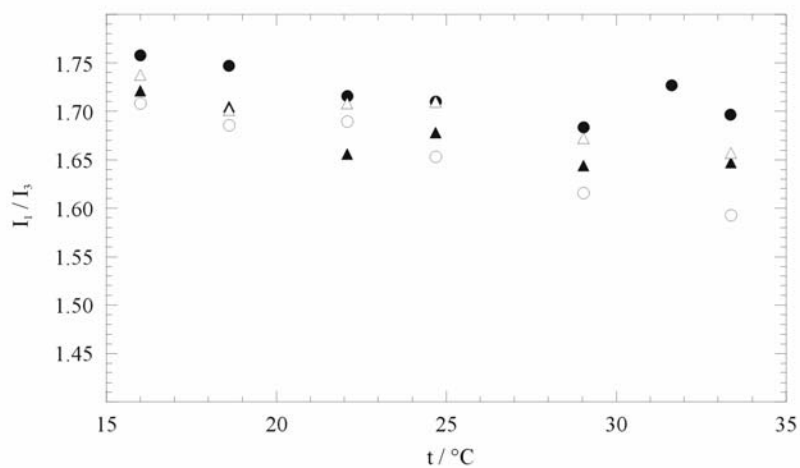


Figure S17. Dependence on temperature of the I_1/I_3 ratio for pyrene fluorescence spectra in water (●) and in the presence of 1,2-dichloroethane at variable compositions: Δ, $m_a=25\text{mm}$; ○, $m_a=50\text{mm}$; ▲, $m_a=60\text{mm}$.

Table S1. Hydrodynamic radii of unimers and aggregates of F108 in water and in water+1,2-dichloroethane.^a

m_p	m_a	$R_{h,u}$	$R_{h,M}$	$R_{h,u}$	$R_{h,M}$	$R_{h,u}$	$R_{h,M}$
		25 °C		30 °C		35 °C	
0.96		3.3		3.4		3.3	14.3
2.44		3.0				2.9	16.7
3.87		2.5		2.7	27.0	3.0	16.3
3.94		2.5		2.6	23.1	3.2	16.0
6.03		2.2	55.0	2.5	28.1	2.8	17.3
6.92		2.2	55.8	2.5	28.0	2.7	17.1
8.24		2.0	62.7	2.4	28.9	2.5	18.0
		25 °C		30 °C		35 °C	
0.96	100	3.4	23.0	3.3	16.0	2.8	13.5
2.44	155	2.5	24.0			2.6	12.7
3.87	97	2.6	35.7	2.8	23.0	3.1	15.5
6.03	102	2.2	45.1	2.6	23.5	2.8	15.9
6.92	104	2.3	40.2	2.5	22.9		
8.24	102	2.1	43.1	2.4	21.5	2.6	18.0

^aUnits are: m_p and m_a , mmol kg⁻¹; R_h , nm.

Table S2. Hydrodynamic radii of unimers and aggregates of L35 in water and in water+1,2-dichloroethane.^a

m_p	m_a	$R_{h,u}$	$R_{h,M}$	$R_{h,u}$	$R_{h,M}$	$R_{h,u}$	$R_{h,M}$
		25 °C		35 °C		45 °C	
0.0496		1.4		1.5		1.9	
0.1013		1.4		1.6			
0.1374		1.5		1.7			
0.2363		1.6	17	2.2		2.7	13
0.3047		2.0	23	2.3	14	2.6	17
0.4398		2.3	29	2.4	30		
0.5788		2.4	45	2.3	38	2.5	37
0.6631		2.4	50	2.3	46	2.3	41
		25 °C		35 °C		45 °C	
0.2363	1.03	2.5	22				
0.3047	1.16	2.7	26			4.2	31
0.4398	1.43	2.4	30	3.2	36		
0.5788	1.17	3.2	45	3.1	41	3.6	41
0.6631	1.19	3.3	55	3.4	44	3.9	43

^aUnits are: m_p and m_a , mol kg⁻¹; R_h , nm.

Table S3. Hydrodynamic radii of unimers and aggregates of 10R5 in water.^a

m _p	R _h		R _h		R _h	
	u	M	u	M	u	M
	25 °C		35 °C		45 °C	
0.0490	1.5		1.5		1.8	
0.1172	1.5		1.9		2.4	
0.1958	1.5		1.9		2.7	9.2
0.2896	1.5		2.0	14	2.7	14
0.3419	1.8	20	2.0	17	3.0	20
0.4613	2.1	28	2.6	25	2.9	24
0.5584	2.7	37	2.6	35	3.2	33
0.6769	2.7	48	2.7	46	3.3	42

^aUnits are: m_p, mol kg⁻¹; R_h, nm.

Table S4. Hydrodynamic radii of unimers and aggregates of F88 in water and in water+1,2-dichloroethane.^a

m_p	m_a	$R_{h,u}$	$R_{h,M}$	$R_{h,u}$	$R_{h,M}$	$R_{h,u}$	$R_{h,M}$
		25 °C		30 °C		35 °C	
1.94		2.8				2.9	
3.62		2.5		2.6		2.8	
5.18		2.3		2.4		2.7	
5.70		2.2		2.4		2.7	21
6.98		2.2		2.3		2.6	21
8.53		1.8		2.2		2.5	24
8.54		2.0		2.2		2.5	25
10.06		2.0		2.1		2.6	26
11.91		1.8		2.0	28	2.7	28
14.92		1.7		2.0	44	2.7	34
		25 °C		30 °C		35 °C	
3.62	108	2.7	15	2.3	11.8	2.0	10.0
5.18	112					2.6	16.0
5.70	105	2.5	17	2.8	12.4		9.4
6.98	105	2.4	18	2.8	13.9		8.0
10.06	103	2.2	25	2.5	15.5		
11.91	108	2.3	23	2.6	18.3	2.9	13.0
14.93	105	2.3	37			2.6	19.7

^aUnits are: m_p and m_a , mmol kg⁻¹; R_h , nm.

Table S5. Critical micellar temperature from fluorescence data for F88 and F108 in water and in the presence of 1,2 dichloroethane at some compositions.^a

	F108				F88	
<i>m_p</i>	0.81	2.08	3.94	4.47	10.06	14.92
	<i>m_a</i> =0				<i>m_a</i> =0	
<i>cmt</i>	29.66	27.05	24.89	31.43	28.69	26.88
	<i>m_a</i> =30				<i>m_a</i> =30	
<i>cmt</i>	23.07	19.20	16.25	25.83	23.52	19.42
					<i>m_a</i> =50	
<i>cmt</i>				24.79	22.79	

^aUnits are: *mm* for *m_p* and *m_a*, °C for *cmt*